Magnesium Technology 2015
Edited by: Michele V. Manuel, Alok Singh, Martyn Alderman, and Neale R. Neelameggham
TMS (The Minerals, Metals & Materials Society), 2015

POWDER METALLURGICAL SYNTHESIS OF BIODEGRADABLE Mg-HYDROXYAPATITE COMPOSITES FOR BIOMEDICAL APPLICATIONS

Cesar Augusto Stüpp[a], Gábor Szakács[a], Chamini Lakshi Mendis[a], Felix Gensch[b], Sören Müller[b], Frank Feyerabend[a], Dachamir Hotza[c], Marcio Celso Fredel[c], and Norbert Hort[a]

[a.] Institute of Materials Research, Helmholtz-Zentrum Geesthacht, Max-Planck-Str. 1, D-21502 Geesthacht, Germany

[b] Forschungszentrum Strangpressen, TU Berlin, Gustav-Meyer-Allee 25, 13355 Berlin, Germany;
[c]Universidade Federal de Santa Catarina, Brazil

Keywords: hydroxyapatite, ball milling, Mg-MMC, bio-corrosion

Abstract

Magnesium alloys with acceptable or even controllable corrosion rates, where mechanical properties are not significantly modified or worsened, have been increasingly investigated in the last decade for use as biomaterials. This work shows an approach with a magnesium metal matrix composite (Mg-MMC), composed of ZK60 as base material and hydroxyapatite (HA) particles. The composite was produced by mechanical alloying followed by hot extrusion, as HA in contact with molten magnesium releases toxic gases such as phosphine (PH_3). This work will present the influence of different amounts of HA on corrosion behaviour and mechanical properties of the investigated composites. Compared to the ZK60 alloy, corrosion is expected to be delayed, without localized corrosion. The mechanical properties are not expected to be compromised with such composite during tissue's healing period.

Introduction

Non-toxicity, degradability, biocompatibility and mechanical properties close to those of bone are reasons why Mg is suitable for biological implant applications [1, 2]. Mg alloys undergo degradation during exposure to physiological conditions, making magnesium an ideal candidate for degradable implants [1]. Mg degradation products can be absorbed, consumed and excreted within a period of time in physiological systems [3]. Additionally, Mg is a common constituent in the human body, where at least half is stored in bone tissues [4]. The high reactivity and rapid corrosion rates observed in Mg can result in loss of mechanical integrity before the surrounded tissue has enough time to heal and bear loads [5].

One approach to solve this problem is the use of Mg metal matrix composite (Mg-MMC), where ceramic particles are distributed within the Mg matrix. Hydroxyapatite (HA) is one such ceramic that is already used in implant applications, as it is biocompatible and bioactive. HA is a constituent of bones and aids osseointegration and cell adhesion [6, 7, 8]. Previous studies have shown that addition of HA reduced the corrosion rates in Mg alloys. Witte et al. [5] reported that adding 20 wt.% HA to AZ91 decreased corrosion rate in artificial seawater. Feng and Han [9] reported a smaller weight loss for ZK60 in physiological saline when reinforced with calcium polyphosphate (CPP).

The biocompatibility of alloying additions is important when choosing alloys for biomedical applications. Both zinc and zirconium are biocompatible. Zinc deficiency causes many physiological functions to be perturbed, such as bone formation, causing metabolic disorders that can result in many diseases [10, 11, 12]. Zirconium is also found in the human body, but its functions are not yet clear [13]. ZK60 has been widely investigated for structural applications and its mechanical and corrosion properties were also investigated [9, 10, 14]. Therefore, ZK60 is a suitable material to be used for the development of biodegradable Mg composite containing HA.

In this contribution we report the findings from an investigation on the ball milled and extruded Mg-6%Zn-0.5%Zr (wt.%) (ZK60) alloy with varying amounts of HA (10 wt.% (6 vol%) and 20 wt.% (13 vol%)). Compression and immersion tests were used to evaluate mechanical properties and corrosion rates along with the microstructure. For easier understanding, the convention ZK60, ZK60-10 and ZK60-20 is adopted for the composite with 0 wt.%, 10 wt.% and 20 wt.% of HA, respectively.

Experimental procedure

ZK60 ingots were cast and machined into millimeter scale chips, and commercially available synthetic HA was used (particle size <42 µm, Alfa Aesar GmbH, Germany). The ZK60 alloy chips and HA were ball milled for 7 hours, at 250 rpm and with a ball to powder ratio (BPR) of 20:1. The powders were hot extruded to produce consolidated material at a temperature of 270 ºC, with an extrusion ratio of 1:10 and speed of 9 mm/s.

Specimens from extruded composites were embedded in epoxy, ground with SiC papers with a grit size from 500 to 2500 and then polished with water-free 0.5 µm colloidal silica solution for optical microscopy and scanning electron microscopy (SEM). Samples for optical microscopy were etched in a solution of ethanol (70%), distilled water (20%) and acetic acid (5%) with addition of 8-9 g of picric acid. SEM investigations were conducted with a Tescan VEGA 3 SEM equipped with an energy dispersive X-ray spectrometer (EDXS).

The compression tests were performed on a Zwick 050 testing machine, with a strain gauge to measure elongations, at room temperature with an initial strain rate of 10^{-3} s^{-1}. The 5 compression specimens of each composite were machined from the extruded bars. Compression samples were 9.5 mm diameter and 17 mm length and prepared according to DIN 50106 [15].

Immersion tests specimens were 8.5 mm diameter and 3 mm thickness and were machined from the extruded rods. These samples were sterilized by autoclaving for 20 min at 121 ºC. Immersion tests were conducted according to the standard ISO 10993-5 [16], for 72 h in 3 ml of Dulbecco's modified eagle medium (DMEM) with 10 vol.% fetal bovine serum (FBS). The

tests were conducted at 37 ºC, with a controlled test environment containing 5% CO_2, 20% O_2, and 95% relative humidity. Following immersion tests, the samples were cleaned in chromic acid (180 g/L) to remove corrosion products and were dried for 24 h at 50 ºC. The weight of the specimens was determined before the immersion tests and after the removal of corrosion products as described above, to determine the corrosion rate for each of the alloys.

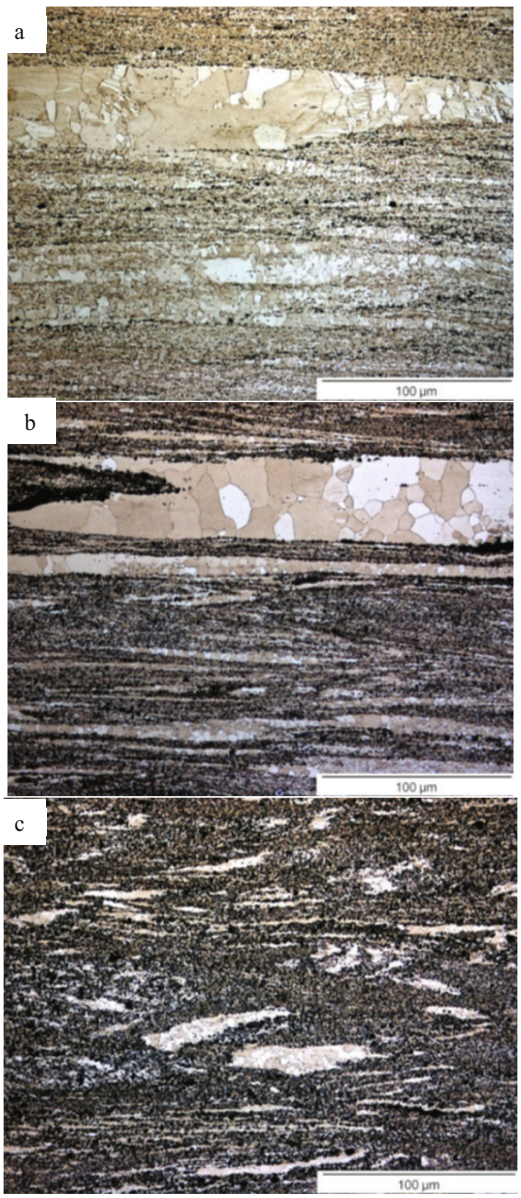

Figure 1: Optical micrographs typical of the ZK60 (a) without HA, (b) with 10 wt.% HA and (c) 20 wt.% HA. Images are parallel to the extrusion direction.

Results and discussion

The optical microstructures of ZK60 with 0, 10 and 20 wt% HA are shown in Figure 1. The microstructures contain a duplex distribution of grains with regions of large grains surrounded by fine grains. The large grained regions occur along the extrusion direction. With the addition of HA, regions of coarse grains decreased and only small regions of coarse grains are observed in ZK60-20. The coarse grain size also decreased with the increase in HA content. In ZK60 and ZK60-10, these grains range from 15 µm to 40 µm, while in ZK60-20, they are less than 20 µm. The fine grained region contained grains that are less than 1 µm. HA is homogeneously distributed throughout the samples, and this distribution causes the formation of fine grains. In ZK60 alloy the fine grained regions are due to the presence of oxide particles introduced during machining and ball milling.

The compression stress-strain curves are shown in Figure 2 and the pertinent features of the stress strain curves are summarized in Table 1. The compression stress-strain curves show that the ultimate strength and yield strength increase with increased HA content, while the elongation decreases. The 0.2% compressive yield strength is 277, 341 and 356 MPa for ZK60, ZK60-10 and ZK60-20 alloys respectively. The increase in yield strength due to HA additions was approximately 60 MPa with 20% HA additions. Elongation to failure changed from 9.6% for ZK60, 6.6% for ZK60-10 and 5.6% for ZK60-20. This is approximately 42% decrease in the elongation to failure from ZK60 with the addition of 20% HA.

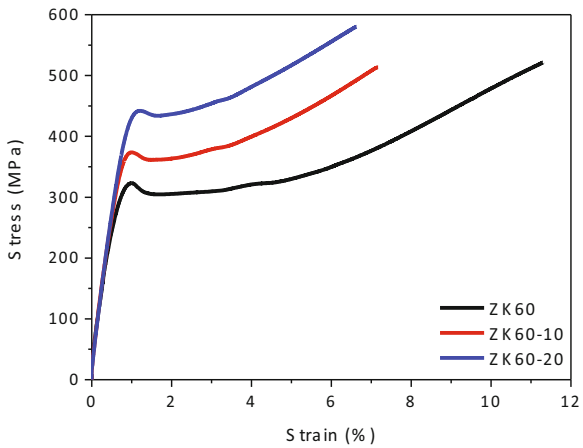

Figure 2: The compressive stress-strain curves of as extruded ZK60 magnesium alloy and ZK60-HA composites.

Table 1: Room temperature compressive properties of ZK60 alloy, ZK60-10 and ZK60-20 composites.

Material	0.2%CYS (MPa)	UCS(MPa)	Elongation (%)
ZK60	277 ± 22	485 ± 35	9.5 ± 1.0
ZK60-10	341 ± 20	529 ± 13	6.6 ± 0.4
ZK60-20	356 ± 54	554 ± 20	5.1 ± 0.4

Table 2: The corrosion rates of ZK60 alloy with 0, 10 and 20 wt% HA additions after immersion in DMEM+10%FBS solution.

Material	Corrosion rate (mm/year)
ZK60	0.50 ± 0.16
ZK60-10	0.47 ± 0.14
ZK60-20	0.41 ± 0.10

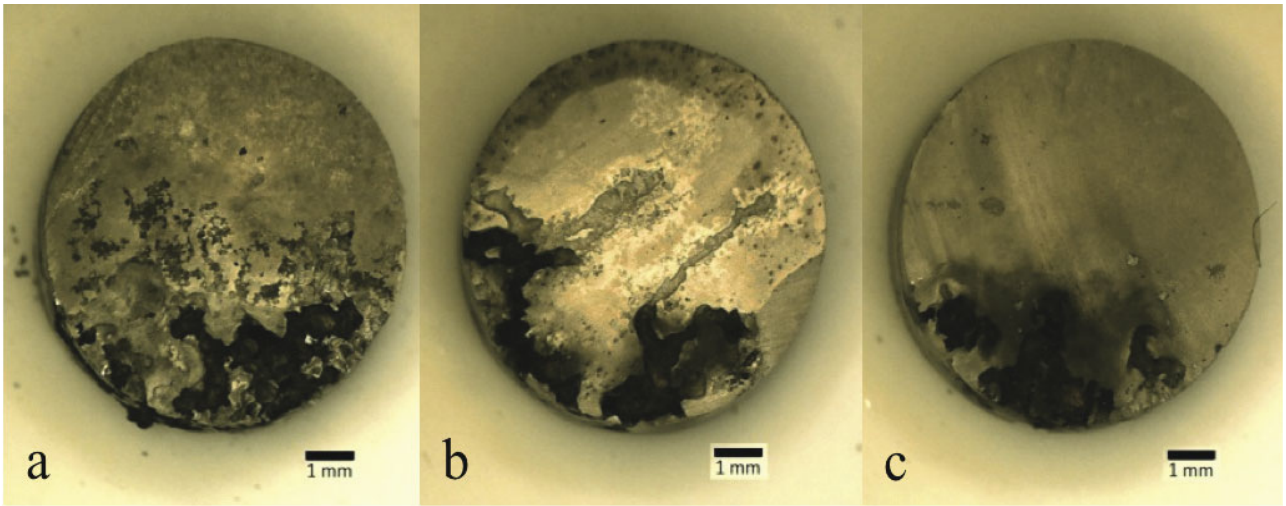

Figure 3: Mg-MMC samples after 72 h immersion in DMEM + 10 vol.% FBS: (a) ZK60, (b) ZK60-10 and (c) ZK60-20.

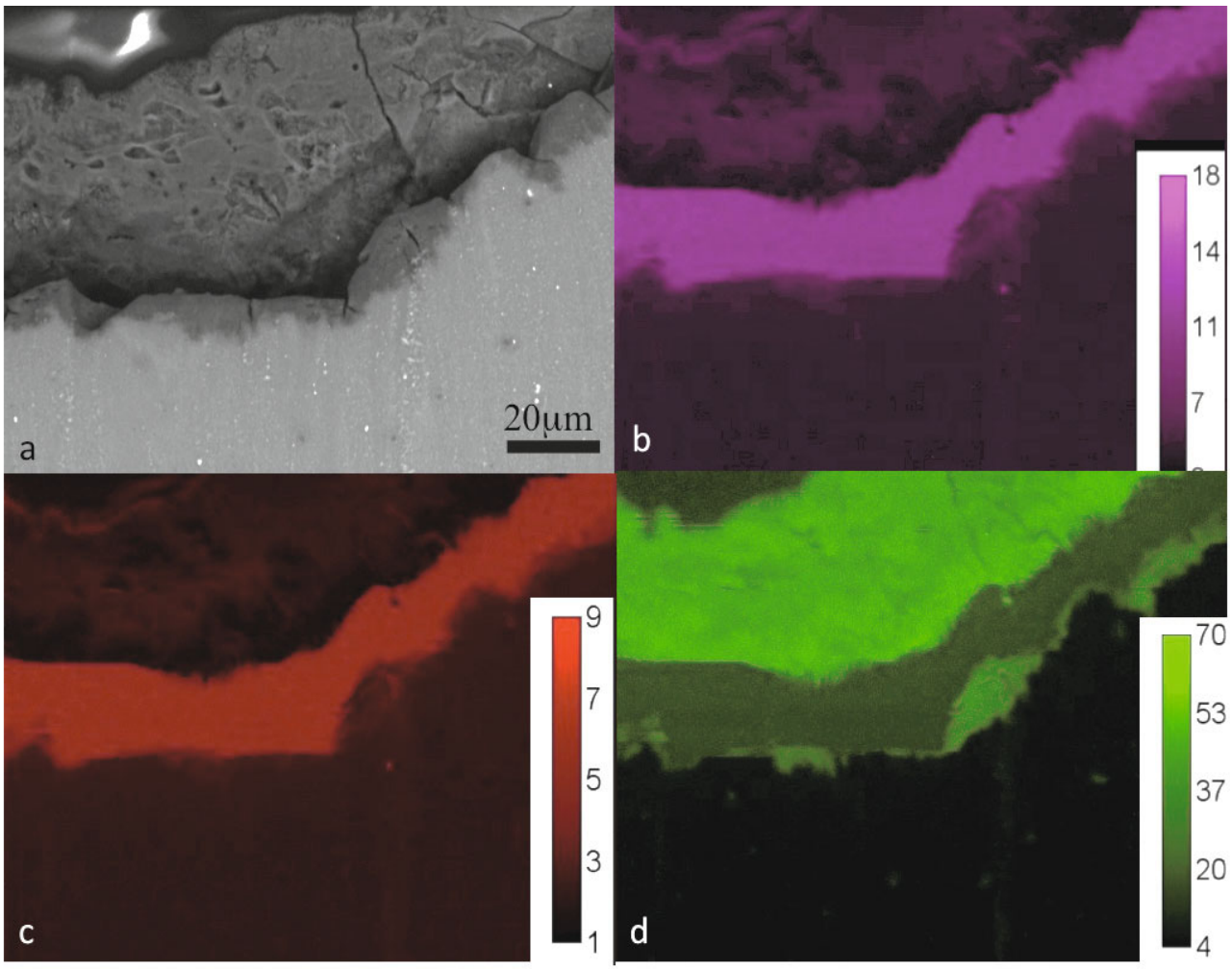

Figure 4: (a) SEM backscattered image of ZK60 alloy after 72h immersion in DMEM + 10 vol.% FBS, showing corrosion product formation and EDX elemental maps showing the (b) Ca, (c) P and (d) O distributions.

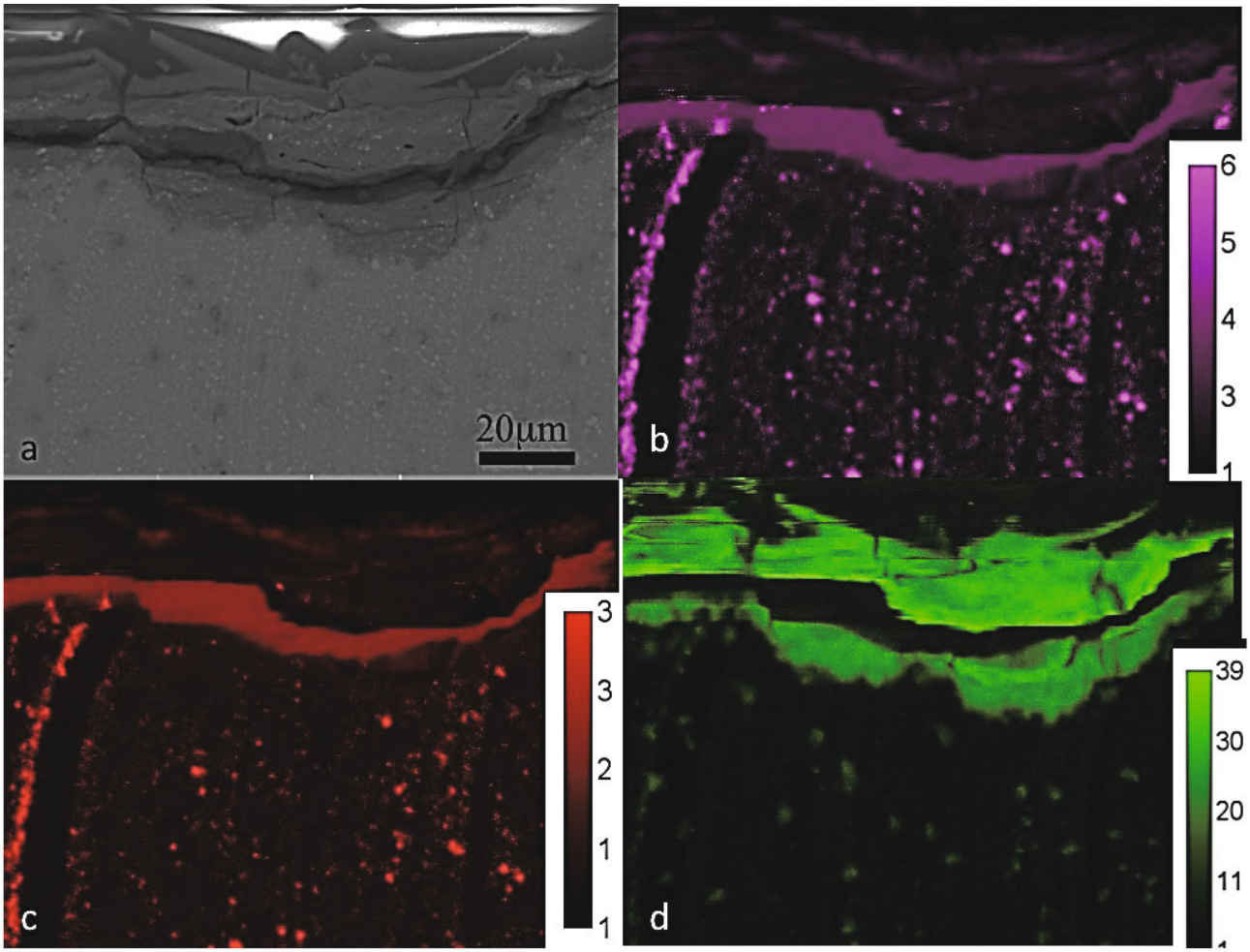

Figure 5: (a) SEM backscattered image of ZK60-10 alloy after 72h immersion in DMEM + 10 vol.% FBS, showing corrosion product formation and distribution of HA; and EDX elemental maps showing the (b) Ca, (c) P and (d) O distributions.

The corrosion rate of the ZK60 alloy decreased with the addition of HA, with 20% HA containing alloy showing the lowest corrosion rate. This is similar to the previous observations [9] on ZK60 alloy containing CPP and AZ91 with HA in artificial seawater [5]. However, this result is contrasted with the results for pure Mg where an increase in the corrosion rate was detected with the addition of HA [17]. These results are shown in Table 2. Figure 3 shows ZK60 samples with various amount of HA after immersion tests showing the corrosion products on the surface of the samples. The corrosion on these samples is not uniform and there is severe localized corrosion in all three samples. The area fraction covered by the localized corrosion seems to decrease with the addition of HA, with 20% HA containing sample showing the least amount of localized corrosion. The reasons behind the localized corrosion are not clear and thought to be due to break down of the very thin oxide layer that formed during autoclaving.

The cross sections corresponding EDX elemental maps showing corrosion product build up in samples immersed in DMEM + 10% FBS solution for ZK60 and ZK60-10 are shown in Figures 4 and 5. The corrosion product layer is thicker in the ZK60 (16.21 ± 2.00 µm approximately) compared with ZK60-10 (4.50 ± 1.35 µm approximately), Figures 4 (a) and 5 (a) respectively. The corrosion product observed for both ZK60 and ZK60-10 are similar with the layer closest to the Mg-MMC consists of O while the intermediate layer is enriched with Ca and P. The top most layers consisted of O. In ZK60-10 the distribution of HA particles through the composite as well as in the corrosion product layer can be observed, Figure 5.

Conclusions

The ZK60 magnesium alloy and its composites were successfully manufactured by ball milling followed by hot extrusion. HA particle size decreased substantially after processing, along with the alloy's grain size. Furthermore, particulates are closely bonded to the Mg matrix. The maximum compressive strength was obtained with ZK60-20 and the elongation decreased with the addition of HA. After immersion tests, it is clear that HA addition slightly decreases the corrosion rate of the composite. The corrosion is macro and localized, with the formation of a corrosion layer based on HA constituents (phosphate and calcium).

Acknowledgements

C.S. acknowledges the project BRAGECRIM for the provision of financial support in form of a stipendium provided by CAPES.

References

1. M.P. Staiger et al., "Magnesium and its alloys as orthopedic biomaterials: a review", *Biomaterials*, 27 (2006), 1728-1734.

2. W.F. Ng, M.H. Wong and F.T. Cheng, "Stearic acid coating on magnesium for enhancing corrosion resistance in hanks' solution", *Surface & Coatings Technology*, 204 (2010), 1823-1830.

3. F. Witte et al., "In vitro and in vivo corrosion measurements of magnesium alloys", *Biomaterials*, 27 (2006), 1013-1018.

4. G. Song, "Control of biodegradation of biocompatible magnesium alloys", *Corrosion Science*, 49 (2007), 1696–1701.

5. F. Witte et al., "Biodegradable magnesium-hydroxyapatite metal matrix composites", *Biomaterials*, 28 (2007), 2163-2174.

6. C.P.A.T. Klein et al., "Studies of the solubility of different calcium phosphate ceramic particles *in vitro"*, *Biomaterials*, 11 (1990), 509-512.

7. M.J. Shen et al., "Effect of bimodal size SiC particulates on microstructure and mechanical properties of AZ31B magnesium matrix composites", *Materials and Design*, 52 (2013), 1011-1017.

8. Y. Yun et al., "Revolutionizing biodegradable metals", *Materials Today*, 12 (2009), 22-32.

9. A. Feng and Y. Han, "Mechanical and *in vitro* degradation behavior of ultrafine calcium polyphosphate reinforced magnesium-alloy composites", *Materials and Design*, 32 (2011), 2813-2820.

10. A. Feng and Y. Han, "The microstructure, mechanical and corrosion properties of calcium polyphosphate reinforced ZK60A magnesium alloy composites", *Journal of Alloys and Compounds*, 504 (2010), 585-593.

11. M. Yamaguchi, "Role of zinc in bone formation and bone resorption", *The Journal of Trace Elements in Experimental Medicine*, 11 (1998), 119-135.

12. A.S. Prasad and D. Oberleas, "Zinc: Human nutrition and metabolic effects", *Annals of Internal Medicine*, 73 (1970), 631-636.

13. X. Lin et al., "The in vitro degradation process and biocompatibility of a ZK60 magnesium alloy with a forsterite-containing micro-arc oxidation coating", *Acta Biomaterialia*, 9 (2013), 8631-8642.

14. X. Wang et al., "Microstructure refining and property improvement of ZK60 magnesium alloy by hot rolling", *Transactions of Nonferrous Metals Society of China*, 21 (2011), s242-s246.

15. DIN 50106 Testing of Metallic Materials; Compression Test (1978)

16. ISO10993-5, Biological evaluation of medical devices - Part 5: Tests for cytotoxicity: In vitro methods, International Standards Organization, Geneva (1993).

17. X. Gu et al., "Microstructure, mechanical property, bio-corrosion and cytotoxicity evaluations of Mg/HA composites", *Materials Science and Engineering C*, 30 (2010), 827-832.